Fast Scanning Synchronous Luminescence Spectrometer Based on Acousto-Optic Tunable Filters

DENNIS M. HUEBER, CHRISTOPHER L. STEVENSON,* and TUAN VO-DINH†

Advanced Monitoring Development Group, Health Sciences Research Division, Oak Ridge National Laboratory, Oak Ridge, Tennessee 37831

A new luminescence spectrometer based on quartz-collinear acousto-optic tunable filters (AOTFs) and capable of synchronous scanning is described. An acousto-optic tunable filter is an electronically tunable optical bandpass filter. Unlike a tunable grating monochromator, an AOTF has no moving mechanical parts, and an AOTF can be tuned to any wavelength within its operating range in microseconds. These characteristics, combined with the small size of these devices, make AOTFs an important new alternative to conventional monochromators, especially for portable instrumentation. The relevant performance of the AOTFs (efficiency, bandwidth, rejection, etc.) is compared with that of typical small-grating monochromator.

Index Headings: Synchronous luminescence; Fluorescence; Instrumentation and acousto-optic tunable filter.

INTRODUCTION

An acousto-optic tunable filter (AOTF) is used to isolate one (monochromator) or more (polychromator) wavelengths of light. The wavelength is changed by varying the frequency of a radio-frequency (rf) field applied to a crystal. In contrast to a grating monochromator, an AOTF offers the advantage of having no moving parts, and it can be scanned or slewed at very high rates (ms time scale) without the possibility of error due to gear backlash or other mechanical problems. Since AOTFs with large optical apertures are available, they have been widely applied for spectral imaging. The mechanical simplicity and small size of these devices also make them an attractive new alternative to grating monochromators for use in a portable luminescence spectrometer. This work involves the development of the first AOTF-based spectrometer with synchronous scanning capability.

Molecular luminescence spectroscopy is a common and useful technique for the qualitative and quantitative analysis of samples of a variety of type and origin. In our laboratory we have a particular interest in portable instrumentation for the analysis of environmental samples in the field, and several portable instruments, using conventional light sources[1] or small lasers,[2,3] have been recently developed for this purpose.

In synchronous luminescence (fluorescence or phosphorescence), both the excitation and emission monochromators are scanned simultaneously. The concept, originally introduced by Lloyd,[4] was developed by Vo-Dinh and his co-worker for multicomponent analysis.[5-7] Usually the wavelength difference between the excitation and emission monochromators is kept constant (constant $\Delta\lambda$). Synchronous fluoresence is able to reduce spectral bandwidth and spectral complicity.[5-8]

The use of AOTFs for UV-Vis and fluorescence spectroscopy has recently appeared in the literature.[9,10] Levin[11] and co-workers have described a portable AOTF-based Raman spectrometer, which is also capable of fluorescence measurement. Tran[12,13] and his co-worker have shown that one AOTF can be used as a polychromator when two or more rf signals are simultaneously applied, each signal being modulated at a unique frequency so that the resulting optical signals can be distinguished. The use of these devices in the near-infrared and visible spectral range has also been reported previously, and several reviews have been published.[13,14]

In this work we describe the development of a new portable luminescence spectrometer with single-wavelength and synchronous scanning capability. The prototype instrument was assembled on an optical bread board, and the relevant characteristics of an AOTF were evaluated and are discussed here.

As a first step in the evaluation of the feasibility of a portable luminescence spectrometer, the diffraction efficiency and rejection ratio of an AOTF were estimated experimentally at several wavelengths. These characteristics are used to compare the AOTF to the grating monochromators of the type used in previous portable instruments. Next, a prototype instrument was constructed with an AOTF as an emission monochromator and a HeCd laser as a source to induce fluorescence in several test solutions. The instrument was operated at two scan speeds (400 nm/s and 25 nm/s). Limits of detection are reported and noise sources are evaluated. Finally, a prototype instrument based on two AOTFs was assembled. The first AOTF was used as an excitation monochromator and the second as an emission monochromator.

AOTF Background and Operating Principle. Most AOTFs are based on a tellurium oxide (TeO_2) crystal. Since it has a high acousto-optic figure of merit, TeO_2 is the most common material used for AOTFs operating in the visible and near-infrared. However, many compounds of interest exhibit optimal absorption and fluorescence emission peak values in the ultraviolet, and TeO_2 is not transparent below 350 nm. In contrast, a collinear-quartz AOTF can be useful down to 250 nm. For this reason collinear-quartz AOTFs were used in this study. (In general, noncollinear TeO_2 AOTFs are preferred for the visible spectral range, since they generally have greater diffraction efficiency, require less cooling, and are smaller and lighter. In addition, TeO_2 AOTFs can have larger optical apertures than the collinear-quartz type.)
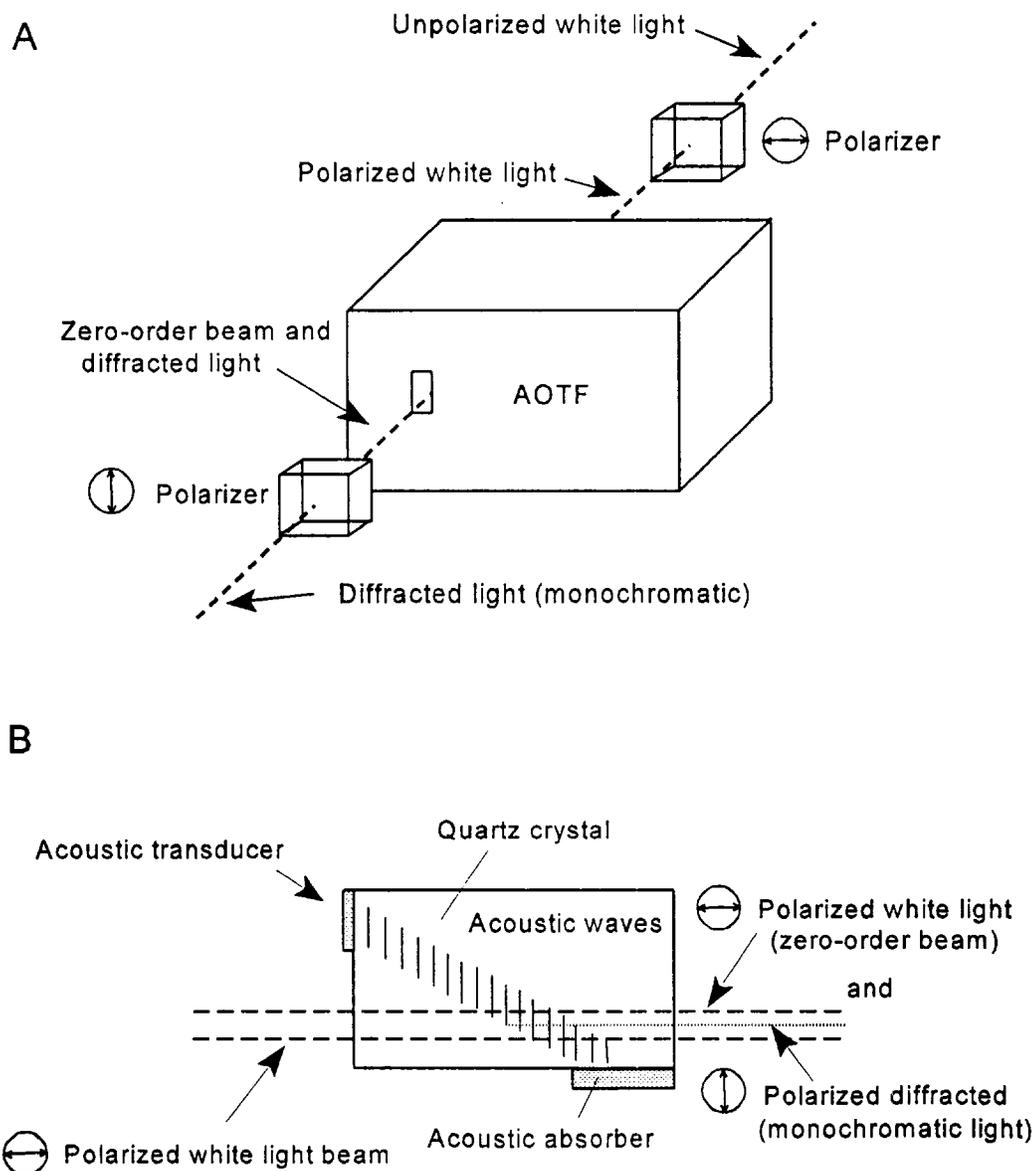
APPLIED SPECTROSCOPY

FIG. 1. The principle of collinear AOTF operation. (A) White light is polarized before entering the AOTF. Both white (undiffracted) and monochromatic (diffracted) light exist in the AOTF before being separated by a second polarizer. (B) Inside the AOTF, light is diffracted by a Bragg diffraction grating established by sound waves within the crystal.

In an AOTF, an rf signal is applied to a piezoelectric driver in contact with a birefringent crystal. The vibration of the piezoelectric driver establishes an acoustic signal in the crystal. The basis of AOTF operation is the Bragg diffraction of light by periodic modulations in the index of refraction in the crystal established by the acoustic waves. Only light within a narrow frequency range is diffracted by this "phase grating".

In a collinear AOTF, the light incident at the optical window in the crystal is linearly polarized. Some of this polarized light is coupled to the diffracted light beam. The polarization of the diffracted (filtered) beam is orthogonal to the incident light. Since the diffracted beam and the incident light beam are collinear, they are separated by a polarizer at the exit of the crystal. Figure 1 is a schematic diagram of a collinear AOTF. The reader interested in the theory of AOTF operation is directed to several articles[15-17] and recent review articles.[13,14]

EXPERIMENTAL

Apparatus. Three different instruments were constructed for this study, as described in the following sections. The same AOTFs, polarizers, PMT, etc., were used for each.

The two quartz AOTFs used in this work were purchased from Brimrose (Model QZAF-.25-.65). According to the manufacturer, the first AOTF had an effective wavelength range of 250 to 650 nm (corresponding drive frequency, 30–175 MHz). The spectral bandpass was 0.1–1 nm and the diffraction efficiency was 25% at 633 nm.

The optical aperture was 2.0 by 5.0 mm, and the acceptance angle was 5° ($\approx f/9$). The second device had the same characteristics as the first except that the diffraction efficiency was less, 15%. Although the two devices were sold as the same model, they were not identical in shape or performance. The more efficient of the two was used whenever only one AOTF was used.

Filters Optical fiber Laser

Polarizers

Lenses

AOTF PMT

Interference filter
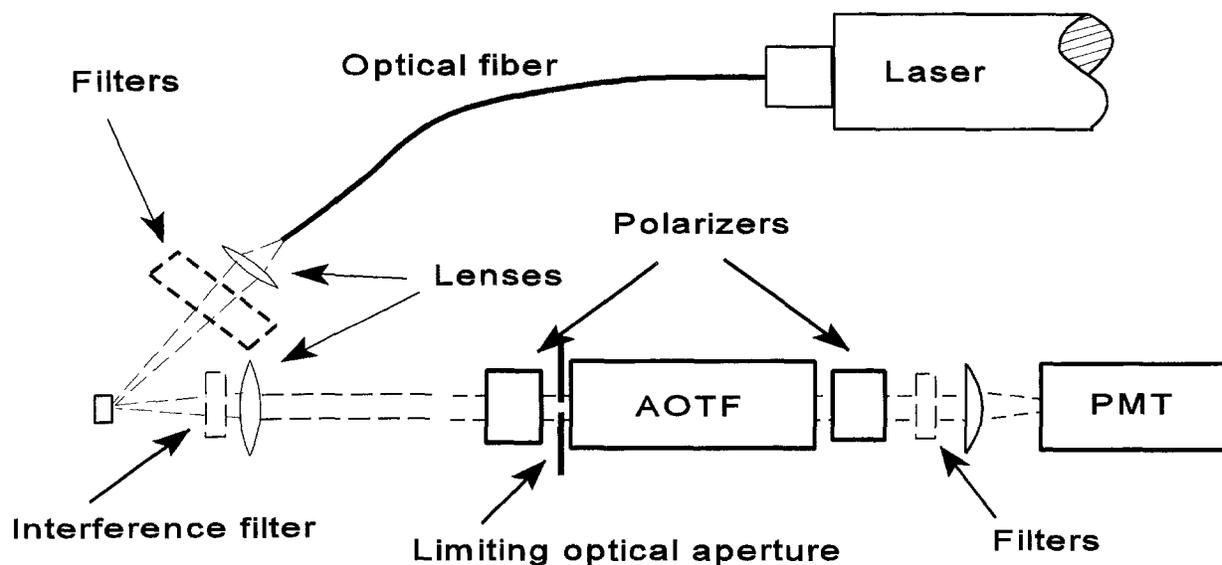
Limiting optical aperture Filters

FIG. 2. Diagram of the system used to measure the AOTF's characteristics.

The rf generator (Brimrose Model AT) could apply 0–25 W of rf power and was controlled by a DOS-based computer using a 16-bit computer controller board supplied by Brimrose. Custom software was developed in the laboratory to control the AOTFs, supporting various scanning modes and fixed-frequency operation.

The PMT was a Hamamatsu R928. The signal from the PMT was conditioned for recording by a laboratory-constructed transimpedance amplifier and lowpass filter (gain 10^8 or 10^9). A 16-bit analog-to-digital converter (Keithly, Model DASH-16) and/or a strip chart recorder were used to record the signal.

All the lenses were quartz and the polarizers were Glen–Taylor types of prism polarizers constructed with UV-transparent epoxy resin (Karl Lambrecht Corp.). One of three lasers or an arc lamp was used as a light source. The arc lamp was a 150-W xenon arc lamp. The three lasers were (1) a HeNe (633 nm, Melles Griot, Model 05-LHP-153), (2) an argon-ion laser (514.5 nm, Coherent, Model Innova 70), and (3) a HeCd laser (325 nm, Omnichrome, Model 3074-6).

Measurement of AOTF Performance. The rejection ratio of the AOTF was estimated at three wavelengths by comparing the intensity of filtered (on-wavelength) to unfiltered (off-wavelength) light transmitted by an AOTF with the use of each of the three lasers in turn. Figure 2 is a schematic diagram of the apparatus used.

A small amount of laser light scattered off a Teflon® target was collimated by a lens and directed toward the first of two polarizers. The polarized light was sent through an AOTF, and a second polarizer was used to block the undiffracted light. A final lens was used to focus the light onto the PMT's photocathode. A 4-mm × 2-mm optical aperture was placed at the entrance of the AOTF to reduce the size of the collimated beam to fit the aperture of the AOTF. This arrangement reduced the amount of light scattered off the edges and sides of the crystal. An interference filter with a peak wavelength matching the laser was placed between the Teflon® target and the collection lens. Each interference filter had a bandwidth of 3–5 nm

and a rejection ratio of at least 10^3. A second interference filter was placed between the AOTF and the PMT.

Neutral-density filters (ND filters) were used to attenuate the laser scatter so that the PMT responded linearly for all measurements. The transimpedance amplifier was used with a very long time constant (10 s), and a strip chart recorder was used to record the signal.

Once the system was carefully aligned with respect to the position of the lenses, the rotation of the polarizers was carefully checked to ensure that the signal from the PMT was minimal when the AOTF was tuned off the laser wavelength. The "off-wavelength" signal was taken as the PMT signal when the AOTF was operated at the full recommended power with a fixed frequency chosen to induce diffraction at a wavelength 15 nm shorter than the laser wavelength. The AOTF was next tuned to the peak of the laser line (ND filters were added as needed), and the "on-wavelength" signal was recorded and normalized to account for the ND filters. The "off-wavelength" signal was equal to the signal present when the AOTF power was turned off, except in the case of the HeNe laser. The rejection-ratio was estimated as the ratio of the "on-wavelength" to "off-wavelength" signals.

To ensure that a high rejection-ratio could be estimated in this manner and to confirm that the quality (extinction ratio) of the polarizers was not the limiting factor, we removed the AOTF from the optical path and measured the ratio of the light intensity transmitted through the pair of polarizers (axes of the polarizers aligned/parallel) to the intensity with polarizers crossed. This ratio should be roughly twice the extinction ratio of one polarizer. At each of the three wavelengths, the estimated polarizer extinction ratio was higher than the estimated AOTF rejection ratio.

The same apparatus was used to estimate the diffraction efficiency of the AOTF. Again the polarizers were adjusted to give the minimum "off-wavelength" signal. The relative intensity of the light transmitted with the AOTF tuned to the maximum laser wavelength and operated at maximum power was measured. Next the AOTF power

Fig. 3 labels: 1 cm quartz cell · Lenses · Optical fiber · Interference filter · Lenses · Filters · Polarizers · AOTF · Lens · PMT
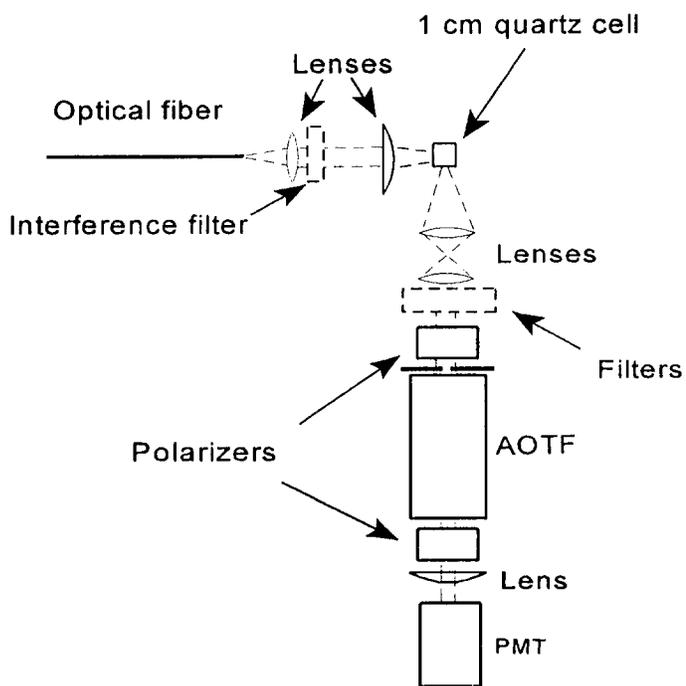
FIG. 3. Diagram of single AOTF spectrometer.

was turned off and the first polarizer was aligned with the second. The signal with the polarizers aligned and the AOTF inactive was recorded. The diffraction efficiency was taken as the ratio of these measurements.

The bandpass of the AOTF was taken as the full width at half-maximum (FWHM) of the apparent laser profile recorded by scanning the AOTF peak wavelength through the region near 633 nm. The manufacturer (Brimrose) measured the bandpass as 0.9 nm at 633 nm in a similar manner. They state that resolution will, in theory, vary from approximately 0.1 nm at 250 nm to 1 nm near 650 nm. A spectrum of a mercury vapor pen lamp was used to calibrate the AOTF drive frequency to the central

wavelength of the AOTF bandpass. The line spectrum of the mercury lamp was also used to measure the approximate resolution of the AOTF. The FWHM of the recorded Hg atomic emission lines varied between 0.3 nm at 296.8 nm and 0.8 nm at 577 nm.

Laser-Induced Fluorescence Measurements with AOTF-Based Detection. Figure 3 is a schematic diagram of the instrument used for emission scans. This apparatus was similar to that described above. Briefly, the HeCd laser was coupled to a 10-m-long, silica-clad/silica-core optical fiber. The laser light emitted (8 mW) from the terminal of the optical fiber was collimated and then focused onto the sample cell by a quartz lens. The fluorescence was collected at a right angle to the excitation beam. An image of the fluorescent spot in the sample cell was formed by the first lens ($f/4$) with 2-to-1 demagnification. A second lens (1.5-cm focal length) was used to collimate the light before it was directed through the AOTF and the second polarizer. Spectral bandpass or neutral-density filters could be placed between the lenses and the first polarizer. Again a rectangular field stop was placed in front of the AOTF to limit the size of the beam incident on the crystal, and a final lens was used to concentrate the light onto the PMT.

Solutions of a variety of fluorescent compounds were made in decade concentration values (10^{-6} M, 10^{-7} . . .) for fluorescence measurements. Each solution was transferred to a clean quartz cuvette (1-cm pathlength) and each emission spectrum was recorded with two scan speeds.

The data acquisition rate was 6000 points/s at 400 nm/s, and 400 points/s at 25 nm/s. The cutoff frequency of the low-pass filter in the transimpedance amplifier was adjusted to $\approx \frac{1}{5}$ of the data acquisition rate to prevent frequency aliasing of excess high-frequency noise. To increase the signal-to-noise ratio, we averaged multiple spectral scans. While 128 of the fast scans were averaged, eight of the slower scans were averaged. The total measurement time was 0.3 s/nm for both cases. After acqui-
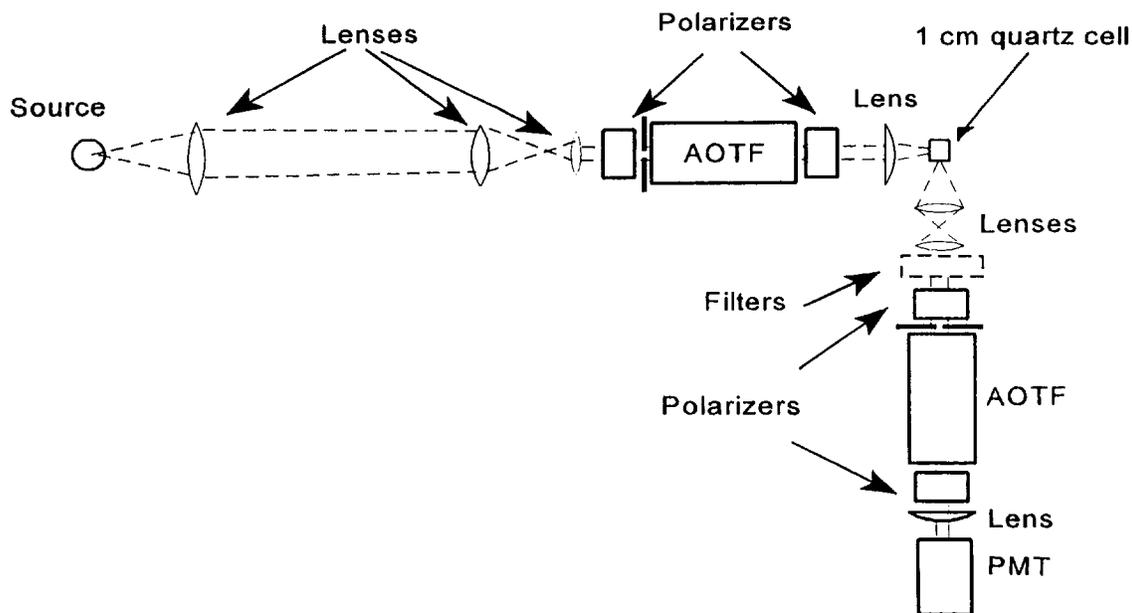
Fig. 4 labels: Lenses · Polarizers · 1 cm quartz cell · Source · Lens · AOTF · Lenses · Filters · AOTF · Polarizers · Lens · PMT

FIG. 4. Diagram of dual AOTF spectrometer.

TABLE I. Estimated diffraction efficiencies and rejection ratios.

Laser (wavelength nm)	HeNe (633)	Argon ion (514)	HeCd (325)
Diffraction efficiency	0.21 ± 3	0.27 ± 4	0.24 ± 4
Est. AOTF rejection ratio	2,050 ± 100[a]	10,700 ± 1000[a]	10,600 ± 1000[a]
	9,800 ± 1000[b]		
Measured polarizer extinction ratio	24,000 ± 1000	26,000 ± 1000	24,000 ± 1000

[a] Based on "off-wavelength" signal.
[b] Based on AOTF power-off signal.

sition, five to six adjacent points in each spectrum were averaged to produce spectra with 0.4 nm/point.

Dual AOTF Spectrometer. Figure 4 is a schematic diagram of the dual AOTF fluorescence spectrometer. The emission part of the instrument is the same as described above. The light from a Xe-arc lamp was collimated by an $f/4/1$-in.-diameter lens. A reduced image of the lamp was formed before it was collimated and directed through an AOTF. The term "collimated" is used loosely here, since simple quartz lenses are not capable of truly collimating white light from an extended source. The lenses were actually adjusted to give a chromatically aberrated image of the source 3 m beyond the AOTF.

RESULTS AND DISCUSSION

Evaluation of AOTF Characteristics. Table I lists the estimated diffraction efficiencies and rejection ratios for the AOTF. The diffraction efficiency values measured were slightly lower than those given by the manufacturer. A high-quality blazed rule grating can have maximum efficiency of 80% in unpolarized light, and a nonblazed holographic grating's efficiency can be 55%.[18] The total efficiency of a small monochromator is typically on the same order as the efficiency of the quartz AOTF.

The rejection ratio was about 10^4 in the ultraviolet and green but only 10^3 at 633 nm. These last measurements were repeated several times, and the results were reproducible. When the AOTF was tuned to 648 nm, it was noticed that the "off-wavelength" signal was much larger than the signal when the AOTF power was turned off (the "power-off" signal). The "off-wavelength" signal was no different from the "power-off" signal in the other cases. Apparently the rejection power of the filter is reduced near the red limit of the spectral range. No manufacturer specification was given for rejection or rejection ratio.

Since a well-collimated monochromatic laser beam was used to measure the rejection ratio, it is possible that a somewhat smaller rejection ratio is actually encountered when the extended broadband source is used. The rejection ratio at 400 nm was approximated with the use of the xenon arc lamp. The rejection was found to be approximately equal to that measured with the UV laser, if the care was taken to block (mask) divergent light before it could enter the AOTF.

The limiting factor for the rejection was loss of polarization due to light scatter of the various surfaces between the polarizers (crystal wall and faces). Any dust on an inside polarizer surface or on the AOTF crystal faces could greatly reduce the rejection power of the filter. In a portable instrument the space between the polarizers should be carefully sealed. The orientation of the polarizers is critical to achieve good rejection. The two polarizers need to be carefully crossed, and they also need to

be aligned with the optical axis of the AOTF crystal. While any quality polarizers (i.e., having $> 10^4$ extinction ratio) will be sufficient, it is important that they be mounted on good rotational mounts. When orientation of the first polarizer was only 0.5° out of alignment with the AOTF, the best rejection ratio was only 10^3. If the error was 2°, the rejection ratio was only 10^2, even when the two polarizers were carefully crossed with respect to each other. In a portable instrument, it may be possible that vibrations would require that the alignment of the polarizers be checked prior to operation at each site.

By comparison, a small-grating monochromator has a stray light rejection ratio of about 10^5. While a rejection ratio of 10^4–10^3 is often sufficient, it is not ideal for molecular fluorescence spectrometry. Consider, for example, an AOTF with a rejection ratio of 10^4 and a source with equal intensity between 200 and 800 nm. The unfiltered light transmitted by the filter would be about 5% as intense as the filtered light. The noise caused by the unfiltered light might preclude the measurement of weakly fluorescent samples, particularly if any specular scatter were present. Bandpass filters could be used to improve the situation, as they often are in grating-based spectrometers.

The spectral resolution of the AOTF is good enough for most molecular luminescence measurements. In fact, lower spectral resolution would be preferable for many luminescence measurements (assuming that the diffraction efficiency was kept constant). A grating monochromator has the advantage of having an easily adjustable spectral resolution.

The optical window of the AOTF (2 mm × 5 mm) is larger than the slit of a small monochromator operated at the same resolution, and the AOTF can filter light entering the front face of the crystal at an angle of 5° to

TABLE II. Comparison between collinear-quartz AOTF-based and small-grating-based monochromators.

	AOTF-based system[a]	Grating-based system[b]
Scan speed	10,000 nm/s[c]	10–100 nm/s
Resolution	≤ 1 nm[d]	Variable
Rejection	10^{-4}	10^{-5}
Optical aperture	Fixed, 2 × 5 mm	Generally >1 mm, depending on resolution
Spectral range	Fixed, 250–650 nm	200–800 nm, depending on grating used
Peak transmission	15–25%	≈50% (at peak wavelength)

[a] Values given for the AOTFs used.
[b] Values given for a typical 0.1 M monochromator.
[c] Wavelength can be set anywhere inside the spectral range within microseconds.
[d] Resolution varies between 0.1 nm at 250 nm and 1 nm at 650 nm. It is not adjustable.
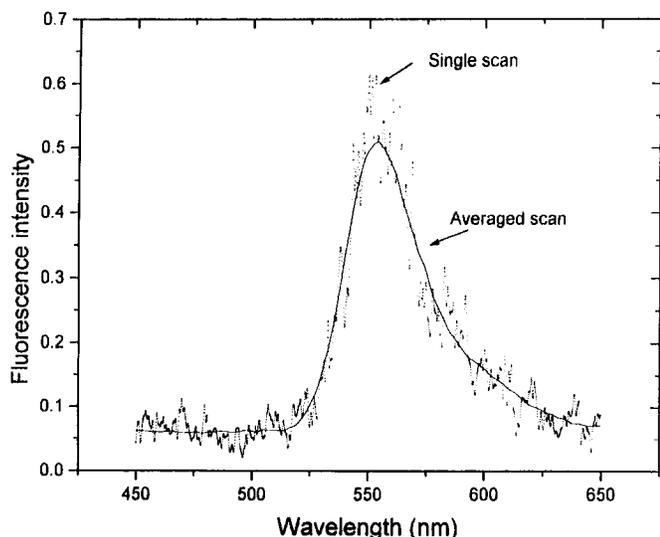
FIG. 5. Emission of spectrum of rhodamine-G (10^{-8} M in ethanol).

FIG. 7. Five spectra of uranine with intensity plotted on a logarithmic scale.

$0°$ (collimated). If a point source of light is considered and optical aberrations are ignored, the AOTF would be capable of accepting a very large (nearly 2πsr) fraction of the total light emitted by the source. A point source could be collimated by an arbitrarily small focal length lens/mirror, thus collecting a large solid angle of light and confining it to a narrow beam of light to be filtered by the AOTF. If an extended source, such as an arc lamp, is collimated, light from various points within the source diverge very quickly and the real collection efficiency is limited and depends on the nature of the source. Smaller sources allow higher solid angles to be collected. Certainly, aberrations in the lenses/mirrors should be considered.

When compared to a small monochromator, the collinear-quartz AOTF transmitted a higher peak spectral radiant power from the same "white" source, but the AOTF's small bandwidth eliminates this advantage for broad excitation and emission bands. Used with 15-nm slits (adequate for most emission or excitation spectra), an H10 monochromator (Instruments SA, Inc.) trans-
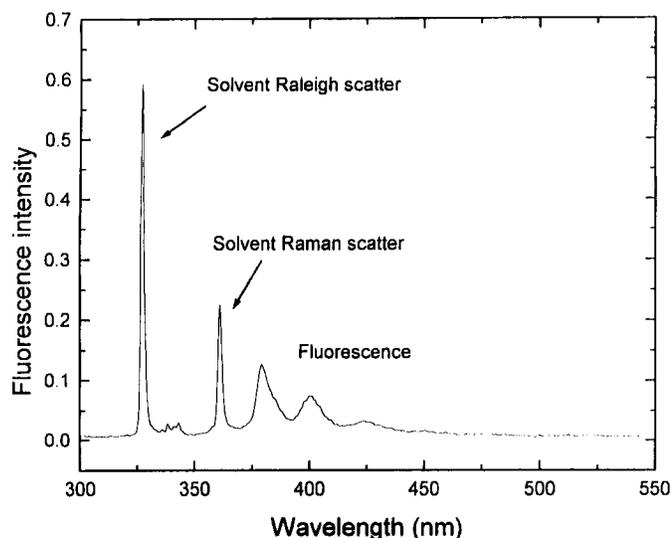
mitted several times greater radiant power. The monochromator's stray light rejection ratio was also higher than the AOTF's rejection ratio. However, the AOTF's advantages of speed and size make it a useful alternative to the grating monochromator. A qualitative comparison between AOTF-based and grating-based monochromators is given in Table II.

Laser-Induced Fluorescence Measurements. Figure 5 shows a spectrum of rhodamine-G (10^{-8} M in ethanol) taken at 400 nm/s. The results with and without spectral averaging are shown. The instrument is capable of very rapid scanning, and spectra can be recorded as a function of time. At low light levels, the increase of the signal-to-noise ratio, owing to the averaging of several spectra, is readily apparent. In response to the concentration of the fluorescent species, the total analysis time can be adjusted from milliseconds to many seconds to achieve the re-
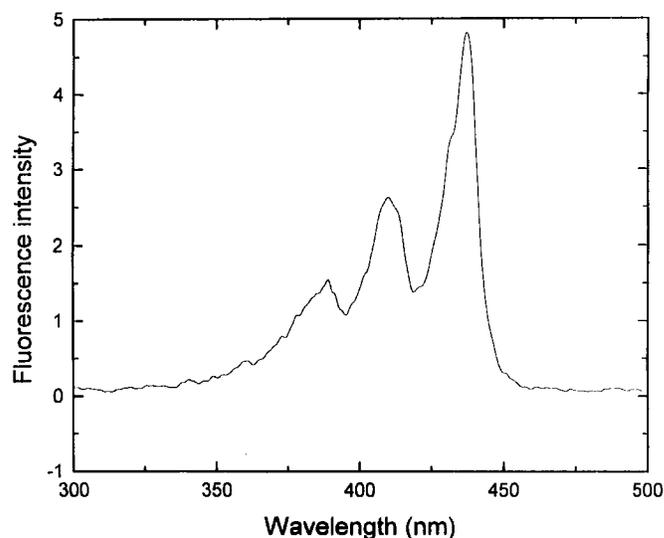

FIG. 6. Emission of spectrum of anthracene (10^{-8} M in ethanol).

FIG. 8. Excitation spectrum of tetracene (10^{-7} M).

APPLIED SPECTROSCOPY **1629**

Compound	Emission max. (nm)	LOD (3σ) (moles/L)
Anthracene	380	3×10^{-10}
Tetracene	512	4×10^{-10}
Uranine	525	1×10^{-10}
Rhodamine-G	560	1×10^{-10}

quired signal-to-noise ratio. One benefit of averaging many rapid scans is that low-frequency noise sources will have little effect on the shape of the resulting spectrum. Also each scan can be stored and displayed, so that the analyst may confirm that each scan is reasonably identical before averaging. Figure 6 shows a spectrum of anthracene (10^{-8} M in ethanol) in which laser scatter and solvent Raman scatter can be seen, and Fig. 7 shows spectra recorded for five concentrations of uranine.

Figure 8 shows an example of an excitation spectrum taken with the same AOTF used as an excitation monochromator and a small (0.10 m)-grating monochromator used as an emission filter, demonstrating the versatility of the AOTF. The source was a xenon arc lamp, and the spectrum is not corrected for the spectral intensity distribution of the source.

Table III lists the limits of detection (LOD) estimated for a variety of compounds. The limits of detection are similar for each compound studied. The detection limits were not significantly different with the slower scan rate (25 nm/s) with proportionately reduced averaging. The limiting noise source was source scatter. Between 350 and 650 nm, the source scatter noise (one standard deviation) from an ethanol blank was ≈ 200 pA (at the PMT). The dark noise (source blocked) was 50 pA. The analog-to-digital converter had an excess noise of 0.0002 V (corresponding to an equivalent PMT noise of 20 pA) electronic interference inside the computer case. It was later determined that the source of this noise was the AOTF controller board(s) within the computer. In future instruments an external ADC could be chosen to avoid this source of noise. A cutoff filter could also be used to reject the laser scatter before the PMT.

Dual AOTF-Based Spectrometer. The instrument was used for rapid excitation, emission, and wavelength synchronous scanning. This work involves the first AOTF-based spectrometer capable of synchronous scanning. An example of a synchronous spectrum of fluorescein is shown in Fig. 9. This spectrum was taken with a scan speed of 400 nm/s and a $\Delta\lambda$ of 20 nm. The capability of the instrument to perform rapid synchronous scans is important, because synchronous luminescence often provides superior selectivity in comparison to excitation or emission spectra. Because of this greater selectivity, more complicated mixtures may often be analyzed and less sample pre-treatment may be necessary.

To help elucidate the performance of the AOTF(s) at the far red end of their spectral response, we took several control spectra. While the first AOTF (the excitation monochromator) was held at a constant wavelength, the second AOTF was scanned over the bandpass of the first. A PTFE target was placed in the sample holder to scatter some of the filtered source radiation through the second
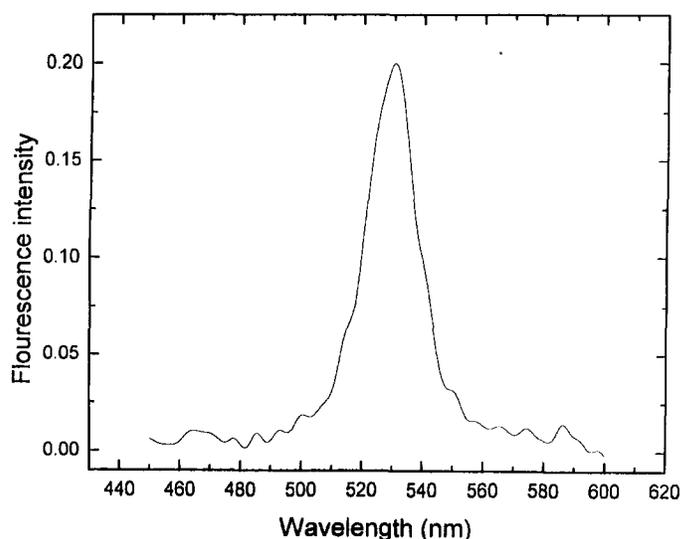

FIG. 9. Synchronous spectrum of fluorescein with $\Delta\lambda$ of 20 nm.

AOTF. This arrangement resulted in a spectrum of the bandpass of the first AOTF. The process was repeated at several wavelengths. Figure 10 shows some of the resulting spectra. Not only does the efficiency of the devices fall off rapidly, but below 635 nm the effective rejection of the system is decreased.

CONCLUSION

The results obtained from a laboratory prototype AOTF-based fluorescence spectrometer are encouraging. The AOTFs tested in this work were efficient and had very good spectral resolution. The AOTFs were easily controlled by software, and several scan modes were developed. Additional modes of operation such as energy synchronous scanning, "slew" scanning, and derivative scanning can be easily added. The speed of the AOTF
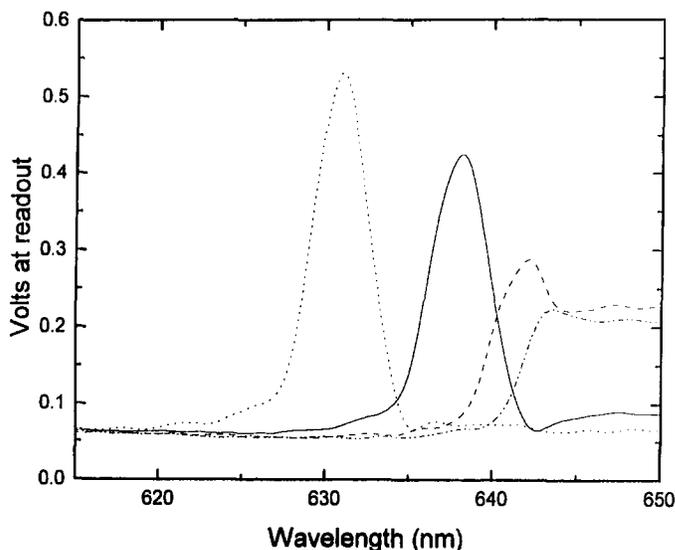

FIG. 10. Spectra of source (Xe arc lamp) light filtered through an AOTF set at several wavelengths near the red limit of the AOTFs spectral range. The first AOTF was used to filter light from the xenon arc lamp at a fixed frequency, and the second AOTF was scanned to take a spectrum of the light passing through the first AOTF. The process was repeated for several fixed wavelengths.

can be particularly useful in environments with excess low-frequency noise, or when kinetic information (on a millisecond time scale) is required. Since the AOTFs can also be operated as fast shutters (turned on and off in microseconds), the same instrumentation could be used for phosphorescence measurements without the need for a separate shutter.

This study demonstrates the feasibility of the development of a portable dual AOTF-based luminescence spectrometer. The AOTFs used did not have rejection power equal to a typical small monochromator, but with the addition of appropriate bandpass filters, they should be adequate for most measurements. The effective rejection power of the AOTF can be improved by amplitude modulation of the AOTF combined with the phase-sensitive detection electronics.[12,13,19] The AOTFs offer several advantages including small size and fast wavelength scanning. The AOTF device is a relatively new technology, in its early phase of development, and many of its capabilities will be evaluated in future studies.

1. J. P. Alarie, T. Vo-Dinh, G. Miller, M. N. Ericson, S. R. Maddox, and W. Watts, Rev. Sci. Instrum. **64**, 2541 (1993).
2. C. L. Stevenson and T. Vo-Dinh, Appl. Spectrosc. **44**, 128 (1990).
3. C. L. Stevenson, R. Johnson, and T. Vo-Dinh, Biotechniques **16**, 1104 (1994).
4. J. B. F. Lloyd, Nature (Phys. Sci.) **123**, 64 (1971).
5. T. Vo-Dinh, Anal. Chem. **50**, 396 (1978).
6. T. Vo-Dinh, Appl. Spectrosc. **36**, 576 (1982).
7. C. L. Stevenson and T. Vo-Dinh, Anal. Chim. Acta **303**, 247 (1995).
8. T. Vo-Dinh, R. B. Gammage, A. T. Hawthrone, and J. H. Throngate, Environ. Sci. Technol. **12**, 1297 (1978).
9. W. S. Shipp, J. Biggins, and C. W. Wade, Rev. Sci. Instrum. **47**, 565 (1976).
10. I. Kurtz, R. Dwelle, and P. Katzka, Rev. Sci. Instrum. **58**, 1996 (1987).
11. E. N. Lewis, P. J. Treado, and I. W. Levin, Appl. Spectrosc. **47**, 539 (1993).
12. C. D. Tran and R. J. Furlan, Anal. Chem. **64**, 2775 (1992).
13. C. D. Tran, Anal. Chem. **64**, 971A (1992).
14. X. Wang, Laser Focus World, **May** (1992).
15. I. C. Chang, Appl. Phys. Lett. **25**, 370 (1974).
16. J. Yu, T. H. Chao, and L. J. Cheng, Proc. SPIE-Int. Soc. Opt. Eng. **1347**, 644 (1990).
17. P. J. Treado, I. W. Levin, and E. N. Lewis, Appl. Spectrosc. **46**, 2775 (1992).
18. J. M. Lerner, SPIE Periodic Structures, Gratings, Moiré Patterns and Diffraction Phenomena **240**, 82 (1980).
19. C. D. Tran and R. J. Furlan, Appl. Spectrosc. **46**, 1092 (1992).